

# Supramolecular Assemblies of Tripodal Porphyrin Hosts and C<sub>60</sub>

Lok H. Tong,<sup>[a, b]</sup> Jean-Luc Wietor,<sup>[a]</sup> William Clegg,<sup>[c]</sup> Paul R. Raithby,<sup>[d]</sup> Sofia I. Pascu,<sup>\*[b, d]</sup> and Jeremy K. M. Sanders<sup>\*[a]</sup>

**Abstract:** The self-assembly of two tripodal porphyrin hosts in the presence of C<sub>60</sub> in the solid state, has been studied using synchrotron X-ray crystallography, and in solution by using <sup>1</sup>H NMR and fluorescence spectroscopies. The binding affinities, stoichiometries and geometries strongly depend

on the size of the porphyrin host. Intramolecular and/or intermolecular porphyrin–fullerene interactions are ob-

**Keywords:** fullerenes · host–guest systems · porphyrinoids · self-assembly

served in the co-crystallites and in each case, the trimer exhibits a “tweezers-like” structural motif. The solid-state structures of the trimer–fullerene co-crystallites reveal close fullerene–porphyrin and fullerene–fullerene contacts.

## Introduction

The unique properties of porphyrins<sup>[1]</sup> and fullerenes,<sup>[2]</sup> such as tuneable HOMO–LUMO gaps and excited state energies,<sup>[3]</sup> have led to intensive investigations of their electrochemical and photochemical properties.<sup>[4]</sup> Supramolecular interactions between fullerenes and porphyrins have attracted considerable interest in recent years for ordering fullerene materials at nanometer dimensions.<sup>[5]</sup> Attractive interactions between the two chromophoric entities have been employed in the construction of preorganized supramolecular arrays. Various three-dimensional multiporphyrin systems that can be used as scaffolds, such as dendrimers<sup>[6]</sup> and por-

phyrin-appended nano- and microparticles,<sup>[7]</sup> have been employed in the construction of preorganized supramolecular arrays. Self-assembly of porphyrins and fullerenes has also been exploited to fabricate and engineer metal surfaces featuring regular structures with nanoscopic periodicities<sup>[8]</sup> as well as metal-organic frameworks containing fullerenes.<sup>[9]</sup> Further supramolecular interactions such as metal–ligand bonding<sup>[10]</sup> and C–F...H–C and C–F...π interactions<sup>[11]</sup> have been engineered in recently to afford additional geometrical control.

The surprisingly close contacts observed between the porphyrin planes and fullerenes in the solid state<sup>[12,13]</sup> have generated considerable efforts towards the design of preorganized porphyrin hosts suitable for strong complexation of fullerenes in solution.<sup>[14–19]</sup> In most cases, two porphyrins complex one C<sub>60</sub> molecule,<sup>[12]</sup> but systems in which the fullerene is surrounded by three,<sup>[11]</sup> or, transiently, four<sup>[18]</sup> or five<sup>[19]</sup> porphyrins have also been reported. Different approaches to the complexation by two porphyrins held together by various linkers have been pursued by us and others. Mainly two approaches have been used to control the relative orientation of the porphyrins: i) two essentially parallel porphyrins linked by two flexible linkers of variable lengths,<sup>[14]</sup> and ii) two porphyrins held parallel or at an angle by a rigid linker.<sup>[15,16]</sup>

The main objective of this work was to assess the role of tripodal hosts (as opposed to the well-studied “porphyrin tweezers”) in the recognition of fullerenes in solution and in the solid state, and to explore the effects of host design on the supramolecular behavior of molecules.

[a] Dr. L. H. Tong, Dr. J.-L. Wietor, Prof. J. K. M. Sanders  
Department of Chemistry, University of Cambridge  
Lensfield Road, CB2 1EW Cambridge (UK)  
Fax: (+44)1223-336017  
E-mail: jkms@cam.ac.uk

[b] Dr. L. H. Tong, Dr. S. I. Pascu  
Chemistry Research Laboratory, University of Oxford  
Mansfield Road, OX1 3TA Oxford (UK)  
Fax: (+44)1865-272690  
E-mail: sofia.pascu@chem.ox.ac.uk  
s.pascu@bath.ac.uk

[c] Prof. W. Clegg  
Department of Chemistry, University of Newcastle upon Tyne  
NE1 7RU Newcastle upon Tyne (UK)

[d] Prof. P. R. Raithby, Dr. S. I. Pascu  
Department of Chemistry, University of Bath  
BA2 7AY Bath (UK)

Supporting information for this article is available on the WWW under <http://www.chemeurj.org/> or from the author.

In this paper, we report the solid and solution state binding behavior of two rotationally flexible tripodal porphyrin hosts **1** and **2** (Figure 1).<sup>[20]</sup> The sole difference between the “large trimer” **1** (i.e.,  $n=1$ ) and the “small trimer” **2** (i.e.,  $n=0$ ) is the type of linkage that connects the three porphyrin components to the central benzene core. Although the

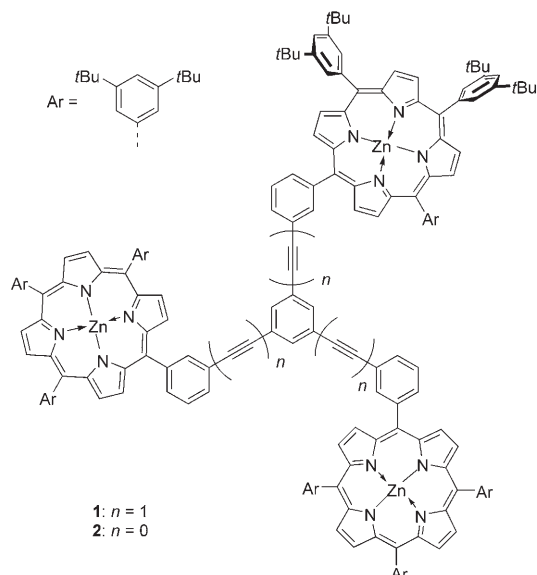


Figure 1. Structure of the tripodal porphyrins employed in this study.

linker in trimer **1** has previously been shown to provide good geometrical features compatible with  $C_{60}$  complexation (Figure 2a),<sup>[17]</sup> the trimeric nature of our molecules raises a number of questions: a) What is the role of the third porphyrin? Does it intervene in a “bridging” complexation mode between two trimer molecules? If so, b) is this interaction precluded in solution due to the high entropic cost involved? c) Does **2**, due to its short interplanar distance, not bind  $C_{60}$  at all? Or d) could it adopt a bowl-shaped conformation that could bind  $C_{60}$  by three porphyrins? e) Will different binding modes be observed in solution and in the solid state?

The large scale syntheses of the two tripodal porphyrins **1** and **2** have been previously reported by our group.<sup>[20]</sup> Here, the solid-state behavior of the tripodal trimers with  $C_{60}$  was probed by co-crystallization of porphyrin and fullerene and their solution behavior was studied by  $^1\text{H}$  NMR and fluorescence spectroscopies. The extremely large size of these supramolecular systems pushed the boundaries of conventional small-molecule crystallography and a synchrotron radiation source was required for the structural analysis.

## Results and Discussion

**Large trimer/ $C_{60}$  co-crystallite 3:** Slow diffusion of hexane into the toluene solution of a 1:2 mixture of **1** and  $C_{60}$  af-

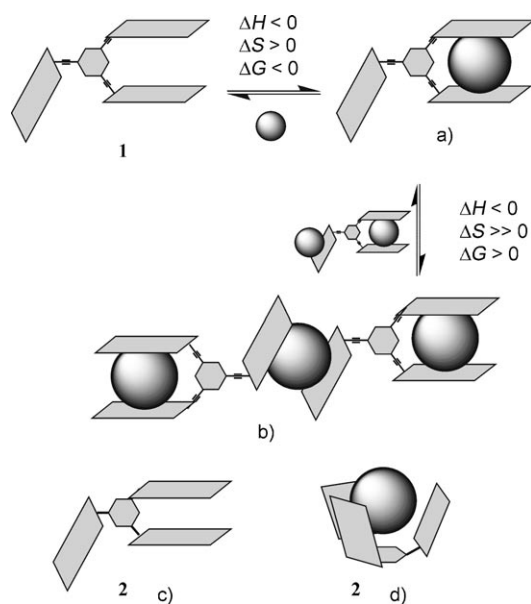


Figure 2. Cartoon representation of possible binding modes of tripodal trimers **1** and **2** to  $C_{60}$ .

forded small, weakly diffracting crystals of **3** which were examined by synchrotron X-ray radiation. Figure 3, which includes the labeling scheme used, shows the schematic representation of the supramolecular complex **3** (**1**: $C_{60}$ ). The asymmetric unit of **3** contains two independent zinc trimers **1a** and **1b** and four crystallographically unique  $C_{60}$  molecules (Figure 3). There are also molecules of toluene and hexane and two zinc-coordinated  $\text{H}_2\text{O}$  molecules in the structure. Except for the axially bound  $\text{H}_2\text{O}$  molecules, all other solvent molecules are disordered and have been idealized during the refinement.

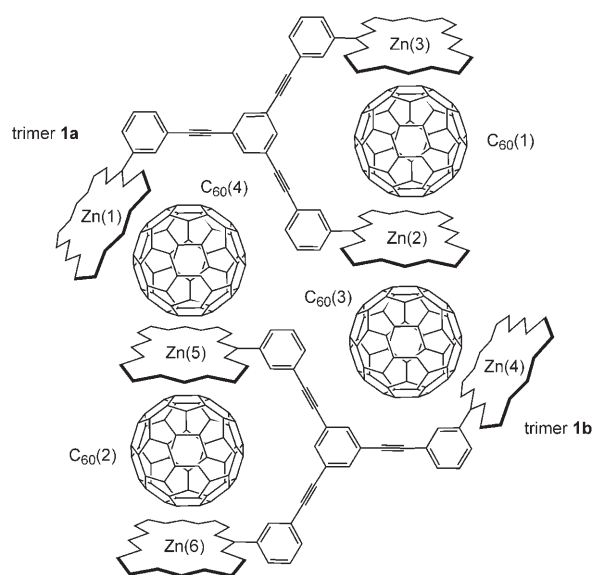


Figure 3. Schematic representation of the main components of the asymmetric unit of the large trimer/fullerene complex **3**.

The two symmetrically unique porphyrin trimers **1a** and **1b** display similar conformations. The U-shaped conformation of two of the porphyrin arms in each trimer intercalates in a tweezers-like arrangement a  $C_{60}$  molecule, whereas the remaining porphyrin unit bends to one side relative to the tweezers motif. The arrangement of the two trimers is such that two additional cavities are created for intermolecular confinement of fullerenes. This compact structure of the fullerene-containing dimer of trimers of **1** has nanoscale dimensions, as characterized by the Zn(1)–Zn(4) and Zn(3)–Zn(6) distances of 27.23 and 37.54 Å, respectively. The 25-atom porphyrin core of each of the porphyrin units is slightly domed and ruffled, with out-of-plane displacement of the metal centers (Table 1).

Table 1. Significant parameters describing the supramolecular architectures of complexes **3** (**1**: $C_{60}$ ) and **4** (**2**: $C_{60}$ ).

Complex	Zn-porphyrin center	Deviation of Zn center from porphyrin best plane <sup>[a]</sup>	Distance of $C_{60}$ center to porphyrin best plane <sup>[a]</sup>	$C_{60}$ radii <sup>[a]</sup>
<b>3</b>	Zn(1)	0.170	6.211 ( $C_{60}$ (4))	3.541
	Zn(2)	0.133	6.136 ( $C_{60}$ (1)), 6.462 ( $C_{60}$ (3))	3.539 ( $C_{60}$ (1)), 3.540 ( $C_{60}$ (3))
	Zn(3)	0.314	6.112 ( $C_{60}$ (1))	3.539
	Zn(4)	0.156	6.182 ( $C_{60}$ (4))	3.540
	Zn(5)	0.146	6.094 ( $C_{60}$ (2)), 6.437 ( $C_{60}$ (4))	3.546 ( $C_{60}$ (2)), 3.541 ( $C_{60}$ (4))
	Zn(6)	0.311	6.069 ( $C_{60}$ (2))	3.546
<b>4</b>	Zn(1)	0.153	6.176 ( $C_{60}$ (1))	3.526
	Zn(2)	0.004	6.199 ( $C_{60}$ (1)), 6.286 ( $C_{60}$ (2))	3.526 ( $C_{60}$ (1)), 3.522 ( $C_{60}$ (2))
	Zn(3)	0.088	6.199 ( $C_{60}$ (2))	3.522

[a] All values quoted in Å.

The tripodal arms in **1a** (containing Zn(2) and Zn(3)) show deviations with respect to the central aromatic plane of 14.0 and 34.3°, respectively. The third arm, bearing Zn(1) gives an angle of 39.3°. The corresponding arms in **1b** (containing Zn(5) and Zn(6)) deviate by angles of 15.4 and 27.2° respectively, whereas the remaining one, bearing Zn(4), shows the greatest deviation from planarity, with an angle of 46.7°.

Two types of binding cavities are observed and all fullerenes are bound by two porphyrin units. The intramolecular, U-shaped binding cavities in **1a** and **1b** are of comparable sizes: the distances between Zn(2)–Zn(3) and Zn(5)–Zn(6) are 12.67 and 12.57 Å, respectively. The U-shaped cavity of both trimers is not composed of two parallel porphyrin planes. Instead tilt angles of 9.2 and 10.7° are observed in **1a** and **1b** respectively. In **1a**, the best planes between the two porphyrins constructing the U-shaped cavity (containing Zn(2) and Zn(3)) and the third porphyrin unit

(containing Zn(1)) form interplanar angles of 51.5 and 59.2°, respectively. Similarly, in **1b**, porphyrins containing Zn(5) and Zn(6) are forming interplanar angles of 51.3 and 59.0°, respectively with the best porphyrin plane containing Zn(4). The two intermolecular binding cavities in the asymmetric unit are also similar. The angle between the porphyrin planes containing Zn(2) and Zn(4) is 51.1°, with a Zn–Zn distance of 11.29 Å. The angle between the porphyrin planes containing Zn(1) and Zn(5) is 51.2°, with a Zn–Zn distance of 11.47 Å.

Rotational disorder of the  $C_{60}$  spheres was observed in this structure. All four  $C_{60}$  molecules in the asymmetric unit are disordered over more than two positions. This is a common feature in the solid-state structure of fullerenes. The disordered  $C_{60}$  units in the structure were idealized and the average refined radii of the  $C_{60}$  molecules are close to 3.54 Å. The fullerenes are centered over the porphyrins in all eight porphyrin–fullerene contacts. The contacts between fullerenes and porphyrin units are characterized by the distances between the best-fit plane of porphyrin units and the surface of the carbon sphere (Table 1). The distances are within the range of 2.52–2.92 Å (Table 1). There are no unbound fullerene molecules in the structure. The fullerene molecules  $C_{60}$ (1) and  $C_{60}$ (3) separated by the porphyrin plane containing Zn(2) have a centroid-to-centroid distance of 12.71 Å. A comparable distance (12.63 Å) is observed for  $C_{60}$ (2) and  $C_{60}$ (4) which sandwich the porphyrin unit containing Zn(5). Other fullerene–fullerene centroid-to-centroid distances are considerable longer.

The relatively long centroid-to-centroid distances in **3** confirm the absence of direct fullerene–fullerene contacts in the crystal. The fullerene molecules  $C_{60}$ (1) and  $C_{60}$ (3) separated by the porphyrin plane containing Zn(2) have a centroid-to-centroid distance of 12.71 Å. A comparable distance (12.63 Å) is observed for  $C_{60}$ (2) and  $C_{60}$ (4) which sandwich the porphyrin unit containing Zn(5). Other fullerene–fullerene centroid-to-centroid distances are considerable longer. The distances of  $C_{60}$ (2) and  $C_{60}$ (3) and  $C_{60}$ (1) and  $C_{60}$ (4) are 14.84 Å and 15.11 Å respectively, and the one between  $C_{60}$ (3) and  $C_{60}$ (4) is 14.66 Å.

The overall crystal structure consists of chains of dimers of trimers (Figure 4), with disordered toluene molecules trapped between the dimeric units and molecules of hexane filling up the voids in the crystal structure. The packing arrangement of the complex **3** suggests no porphyrin–porphyrin, porphyrin–fullerene and fullerene–fullerene interactions between units of different dimeric complexes (Figure 5).

**Small trimer/ $C_{60}$  complex 4:** As with **3**, slow diffusion of hexane into the toluene solution of a 1:2 mixture of **2** and  $C_{60}$  afforded crystals of complex **4**. Figure 6 shows the molecular structure of the 1:2 supramolecular complex **4** (**2**: $C_{60}$ ) as determined by X-ray analysis using synchrotron radiation. The asymmetric unit in **4** contains one porphyrin trimer and two crystallographically unique  $C_{60}$  molecules. A number of solvating molecules are also found in the unit cell. They are all disordered and have been idealized during

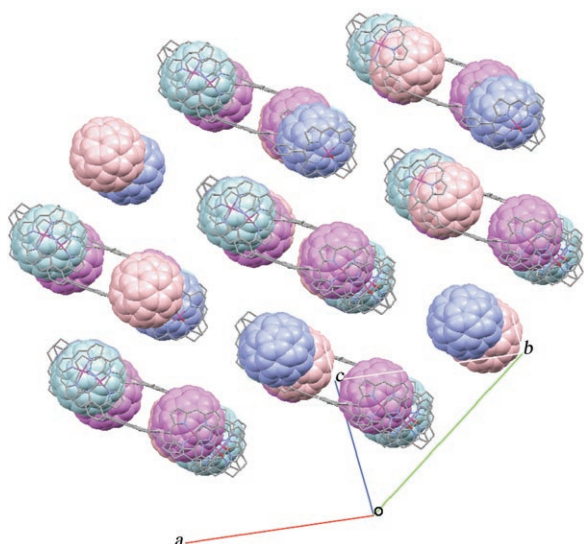


Figure 4. Molecular packing in complex **3** showing the unit cell axes.

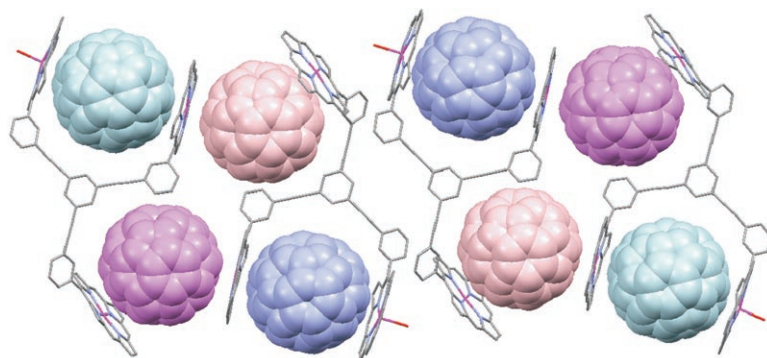


Figure 5. Crystal packing diagram of **3**, showing a fragment of the unit cell.

the refinement. There are no water molecules coordinated to the zinc centers, however.

With respect to the central aromatic plane, the two tripodal arms containing Zn(2) and Zn(3) show deviations of 19.1 and 39.9°, respectively, the third, bearing Zn(1), showing a greater deviation from this plane, by an angle of 37.7°. The best planes between the two porphyrins constructing the U-shaped cavity containing Zn(2) and Zn(3) and the third porphyrin unit (containing Zn(1)) are at angles of 61.7 and 74.6°, respectively.

The small trimer in the asymmetric unit is arranged such that binding cavities suitable for two intermolecularly-bound fullerene molecules are created (Figure 7). Two fullerene molecules are accommodated in binding pockets composed of two tilted porphyrin units, belonging to neighboring trimeric units. The distance between two zinc centers Zn(2)–Zn(3) is 7.10 Å. A toluene molecule (disordered) was found trapped in the U-shaped cavity. The distances of the zinc centers Zn(2) and Zn(3) to the best plane of the intercalated toluene molecule are 2.86 and 2.08 Å, respectively, suggesting possible  $\pi$ – $\pi$  interactions. The angle between the

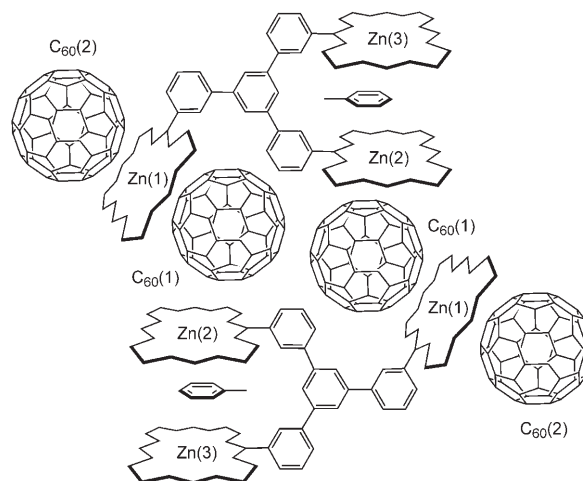


Figure 6. Schematic representation of the main components of the asymmetric unit of the small trimer/fullerene complex **4**.

porphyrin planes containing Zn(3) and Zn(2) is 13.3°. The angle between the porphyrin plane containing Zn(1) of one trimer and the other plane containing Zn(2) of another trimer is 61.7°, with a Zn–Zn distance of 10.85 Å. The angle between the porphyrin plane bearing Zn(1) of one trimer with the plane containing Zn(3) of another trimer is 74.6°, with a Zn–Zn distance of 9.73 Å.

As with **3** the 25-atom porphyrin core of each porphyrin unit in the small trimer is slightly domed and ruffled. The nitrogen atoms are nearly coplanar (maximum deviations from best plane 0.04 Å (ring bearing Zn(1)), 0.06 Å (ring bearing Zn(2)) and 0.15 Å (ring bearing Zn(3))); the zinc atoms are situated at a mean distance of 0.05 Å above the N<sub>4</sub> planes (i.e., Zn(1): 0.01 Å, Zn(2): 0.06 Å and Zn(3): 0.09 Å). These displacements are within the range observed in mononuclear zinc porphyrins.<sup>[21]</sup>

Since all C<sub>60</sub> molecules in the asymmetric unit were severely disordered over more than two positions, a continuous sphere model was attempted initially during the structure refinement.<sup>[14]</sup> However, this did not provide a more suitable final model, and the results of the conventional refinement procedure are reported here. The average radii of the C<sub>60</sub> molecules are close to 3.52 Å in both refinement models. The fullerenes are centered over the porphyrins in all porphyrin–fullerene contacts. The approach of fullerenes to porphyrin units is characterized by the distance between the best-fit plane of porphyrin units and the surface of the carbon sphere. The four contacts span the range of 2.65–2.76 Å (Table 1).

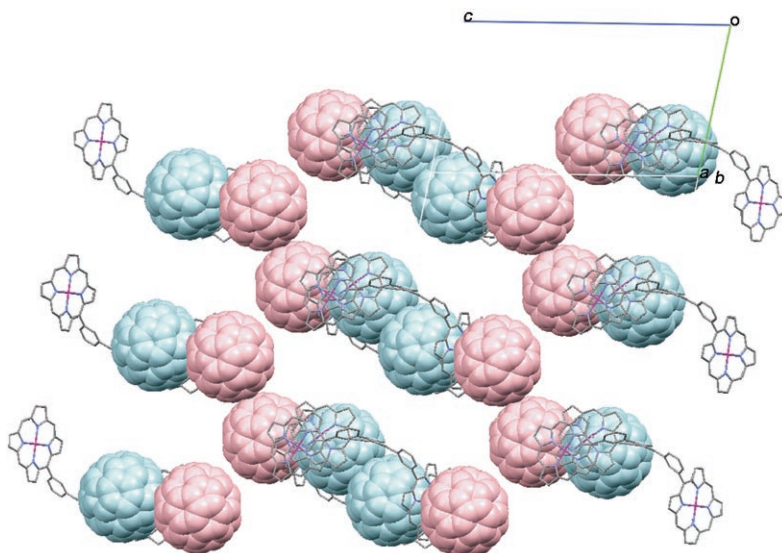


Figure 7. Molecular packing in complex **4** showing the unit cell axes.

There are no unbound fullerene molecules in the structure. All  $C_{60}$  molecules are surrounded by two porphyrins in an inclined fashion as described above. The two symmetry related fullerene molecules  $C_{60}(1)$  are separated by a distance of 10.06 Å. The same fullerene–fullerene contacts are also present between nearby chains. A number of disordered solvating molecules are found in the unit cell. With the exception of the one toluene molecule that is sandwiched in the U-shaped cavity, there are no obvious interactions between toluene molecules and the porphyrin planes. Hexane molecules fill up the voids in the crystal structure.

The overall crystal structure is composed of infinite columns of polymeric chains of the asymmetric unit (Figure 8). Each polymeric chain is surrounded by another six chains of polymer and there are fullerene–fullerene contacts between each polymer and two nearby chains, with a centroid-to-centroid distance of 10.06 Å. No close porphyrin–porphyrin contacts are observed.

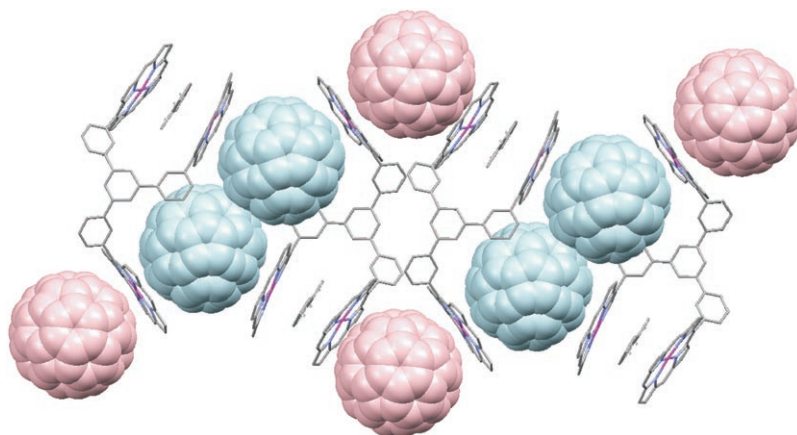


Figure 8. Crystal packing in **4** viewed down the chains of the asymmetric units.

**Structural comparison between **3** and **4**:** The complexes studied exhibit close resemblance in their solid state structure despite their geometrical differences. The “third” porphyrin arm seems to play similar roles in both structures. Two of the three porphyrin arms are engaged in a tweezers-like conformation, allowing the third unit to adjust with respect to the intermolecular binding which brings two tripodal porphyrins together. In the case of **4**, the asymmetric unit is extended to give a polymeric chain whereas in **3** the porphyrin–fullerene interactions yield a discrete dimeric supramolecular entity.

Related dimeric supramolecular complexes of porphyrin oligomers have also been observed in the solid state, for example, in the crystal structures of supramolecular dimers of porphyrin cages assembled via  $\pi$ -interactions between axially coordinated pyridines<sup>[22]</sup> and hydrogen-bonding involving axial methanol molecules.<sup>[23]</sup>

Porphyrin–fullerene interactions seem to provide the driving force for the formation of both solid state assemblies of **3** and **4**. The close proximity of fullerenes to the porphyrin planes suggests an attractive nature of such interactions. This is characterized by the distances between the best-fit plane of porphyrin units and the surface of the carbon sphere (2.70–2.93 Å) which are significantly less than the sum of the van der Waals radii (3.09 Å).<sup>[24]</sup> Combined with the doming or ruffling of all the porphyrin planes, this provides evidence of the van der Waals nature of the attractive forces, where such geometrical distortion of the planar surfaces has often been regarded as the result of maximizing the strength of attractions by wrapping fullerenes more effectively.<sup>[10]</sup>

The porphyrin units in complexes **3** and **4** interact in either 1:1 or 1:2 fashion with fullerenes. This is common to porphyrin–fullerene complexes in solid state as reported in early co-crystallization studies. All fullerenes in both structures are bound by two porphyrin units. The fullerenes in **3** are either encapsulated in the U-shaped cavities or held between two porphyrins at an angle. Only the latter geometry is present in **4**. Inclusion of fullerene by the large trimer in **3** is possible because of its complementary size

of cavity, which can accommodate the spherical guest. On the other hand, the short interplanar distance of the cavity size of the small trimer in **4** frustrates the  $C_{60}$  encapsulation but allows a toluene molecule to be entrapped within  $\pi$ - $\pi$  distance.

The two intermolecular fullerene binding pockets in **3** are strikingly similar, as indicated by their close Zn–Zn separation and the tilt angle between the porphyrin planes. These cavities are comparable to that observed in the “Jaws Porphyrin” host reported by Reed, Boyd and co-workers,<sup>[16]</sup> where the angle between the porphyrin planes is  $42^\circ$  with a metal-to-metal distance of 11.94 Å. The intermolecular binding cavities in **4** are rather different from those in **3**. In addition to the considerably larger angles subtended by two porphyrin planes, the Zn–Zn distances are also noticeably shorter than those in **3**.

The fullerene–fullerene interactions in solid state are commonly described by centroid-to-centroid distances close to 10 Å (the van der Waals limit of the fullerene).<sup>[24]</sup> In **3**, all centroid-to-centroid distances are relatively long, suggesting the absence of such interaction. For **4**, the two symmetry-related fullerenes confined as a pair for interactions in the asymmetric unit show close contact for fullerene–fullerene interactions. A dimeric arrangement of  $C_{60}$  molecules at the van der Waals distance was previously known, such as in the structure of a 1:1 *p*-bromo-homooxocalix[3]arene  $C_{60}$  complex.<sup>[25]</sup>

There are significant conformational differences between the free host **1** observed in the crystal structure previously reported<sup>[20]</sup> and in complex **3**. This reveals the conformation-determining properties of the porphyrin–fullerene interactions. The relatively open and “spread-out” conformation observed for the free host **1** is likely to generate the most effective packing geometry in the absence of the fullerene. The sum of weak solid state forces has been observed earlier to have influences on packing modes and the orientation of flexible organic molecules.<sup>[27]</sup> The distinctive tweezers-like conformation observed for the two crystallographically unique hosts (**1a** and **1b**) in the asymmetric unit of complex **3** is largely dictated by the porphyrin–fullerene attractions, although the intermolecular forces may also influence the overall packing arrangement.

In both cases, the crystals were extremely small and diffracted weakly, and the solving and refining of the extremely large systems pushed the boundaries of conventional small-molecule crystallography. The solving of the two structures was only possible when synchrotron radiation and low temperature was used for data collection. Although the relatively high *R* factors associated with these systems may inevitably limit the precise determination of all structural features, the main part of the porphyrin planes and tripodal linker are extremely well behaved. Disorder mainly affects the solvent molecules and the *tert*-butyl groups at the extremities of the trimers. Therefore, data available should not hinder the validity of our discussion of the intermolecular interactions.

**Solution studies:** The solution behavior of porphyrins **1** and **2** in presence of  $C_{60}$  was monitored by  $^1\text{H}$  NMR and fluorescence spectroscopies. Toluene was the solvent of choice as both fullerene and porphyrin trimers exhibit good solubility, and as it allows comparison with most published studies. Other solvents tend to artificially exaggerate the binding affinity due to insufficient solubility of the fullerene (e.g.  $\text{CHCl}_3$ ) or weaker porphyrin–fullerene interactions,<sup>[14b]</sup> because of too strong competition by the solvent. In, for example,  $\text{CS}_2$ , no binding could be detected.

Steady-state fluorescence spectroscopy ( $\lambda_{\text{ex}} = 420 \text{ nm}$ ) showed the reduction of emission intensity upon adding the guest. After adding 100 equivalents of guest to a  $7.5 \mu\text{M}$  solution of **1** or **2** in toluene, emission intensity dropped to about half of its original intensity (Figure 9). At higher concentrations, qualitatively full quenching of fluorescence was observed when a small excess of fullerene was added. This qualitative observation is indicative of close porphyrin–fullerene contacts in both cases. The Soret band of **1** displayed a bathochromic shift (see Supporting Information), which likewise was too slight to allow calculation of binding data.

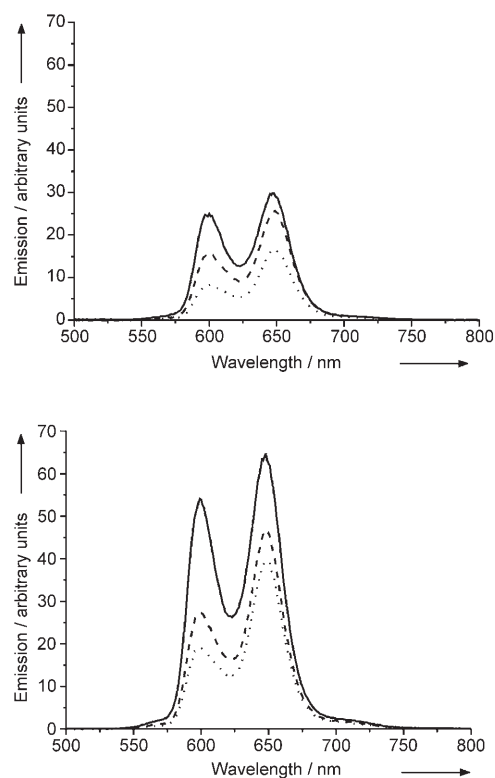


Figure 9. Fluorescence quenching of **1** (top) and **2** (bottom) ( $7.5 \mu\text{M}$  in toluene, room temperature) upon addition of  $C_{60}$ ; —: 0 equiv, ----: 55 equiv, .....: 100 equiv.

$^1\text{H}$  NMR titrations of the large trimer **1** with  $C_{60}$  in  $[\text{D}_8]\text{toluene}$  (see Supporting Information) displayed significant shifts of most of the proton resonances (Figure 10a). A Job plot showed a clear stoichiometry of 1:1 for host **1** to  $C_{60}$ . Binding constants were calculated for a 1:1 binding

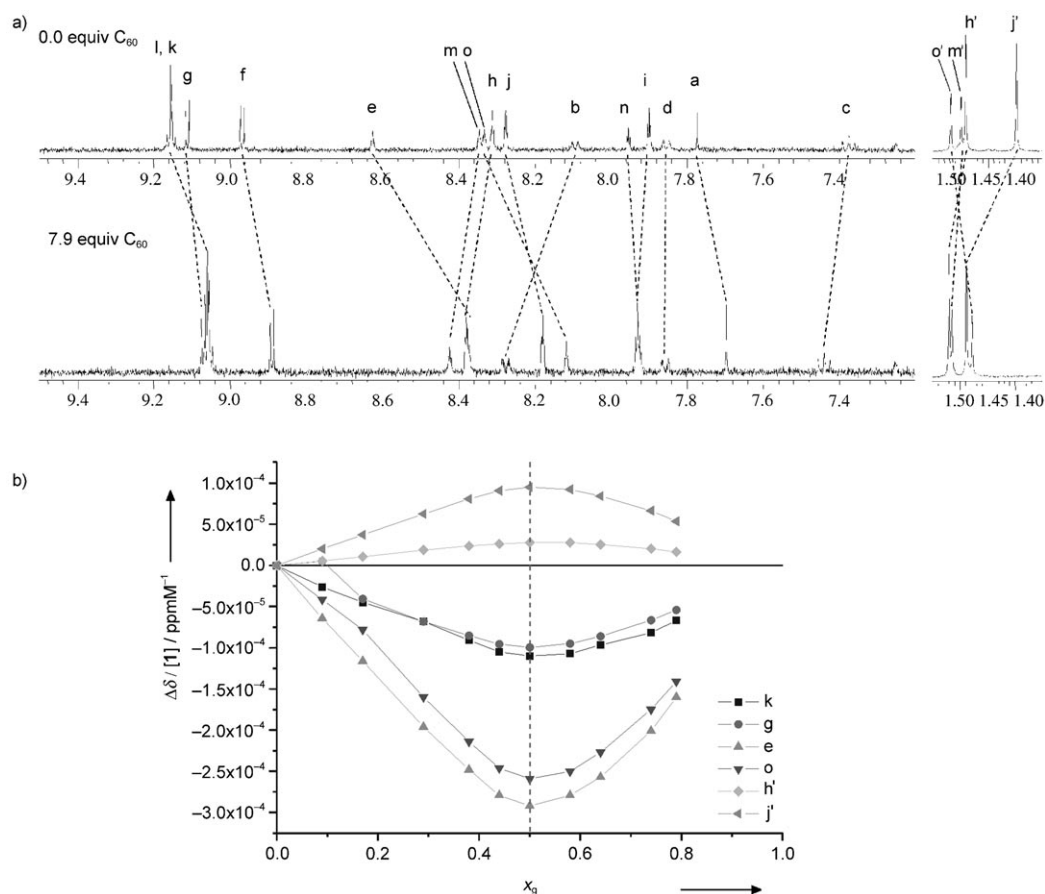


Figure 10. Titration of **1** ( $4.0 \times 10^{-4} \text{ M}$  in  $[\text{D}_8]$ toluene, constant concentration, 300 K) by  $\text{C}_{60}$ . a)  $^1\text{H}$  NMR chemical shift changes, b) Job plot for selected proton signals.

model by fitting an ideal binding isotherm to the experimental data. Most proton signals allowed good fitting, and association constants were found to be about  $2500 \pm 300 \text{ M}^{-1}$  at 300 K, which is in the range of the affinities reported by others for related systems under similar conditions.<sup>[17]</sup>

Less dramatic shifts were observed upon addition of  $\text{C}_{60}$  for the small trimer **2** (see Supporting Information) than in the case of the large trimer **1** (Figure 11). Nevertheless, several protons experience significant upfield shifts. Binding constants calculated from the upfield-shifted signals range from about 300 to  $1000 \text{ M}^{-1}$ . A Job plot performed on the upfield-shifted signals shows a clear 1:1 binding ratio. However, the same Job plot titration showed that downfield-shifted protons suggest a stoichiometry of 2:1  $\text{C}_{60}$ :**2**. Conversely, binding constants calculated from most downfield-shifted protons are situated in the range of  $200\text{--}300 \text{ M}^{-1}$ . The binding isotherm found for proton *a* (Figure 12) bears the clear signature of a process involving two separate binding events. We were not able to fully explain the nature of this second binding event. Potentially more informative variable temperature NMR studies were precluded by insufficient solubility of the analytes at low temperatures.

Solution-state binding modes were deduced from the chemical shift changes measured upon guest binding.

Figure 13 depicts pictorially the chemical shift changes experienced by **1** and **2** upon complexation of  $\text{C}_{60}$ . According to Figure 13a, it can be assumed that in the **1**: $\text{C}_{60}$  complex the  $\text{C}_{60}$  molecule is situated centrally above the porphyrin plane. Given the increasing differentiation of the protons above and below the porphyrin plane it seems reasonable to assume that only one of the faces of each porphyrin is involved in this binding event. This hints at a tweezers-like binding mode (as depicted in Figure 2a), where the third porphyrin in the trimer would remain unbound in solution. In the complex of trimer **2** and  $\text{C}_{60}$ , most upfield shifted signals belong to protons situated at the end opposite the central linker (Figure 13b). This result can be explained by a  $\text{C}_{60}$  binding to the rim of a bowl-shaped conformation of the porphyrin trimer, such as depicted in Figure 2d. Indeed, the ca.  $12 \text{ \AA}$  cavity (as estimated by PM3 modeling for the bowl-like conformation of the small trimer **2** reported by us earlier)<sup>[20]</sup> would be well-suited to encapsulate one  $\text{C}_{60}$  molecule. It is not surprising that this binding mode was not observed by X-ray diffraction, given that the entropic penalty for an intermolecular complexation (type b, Figure 2) is largely reduced in the solid state.

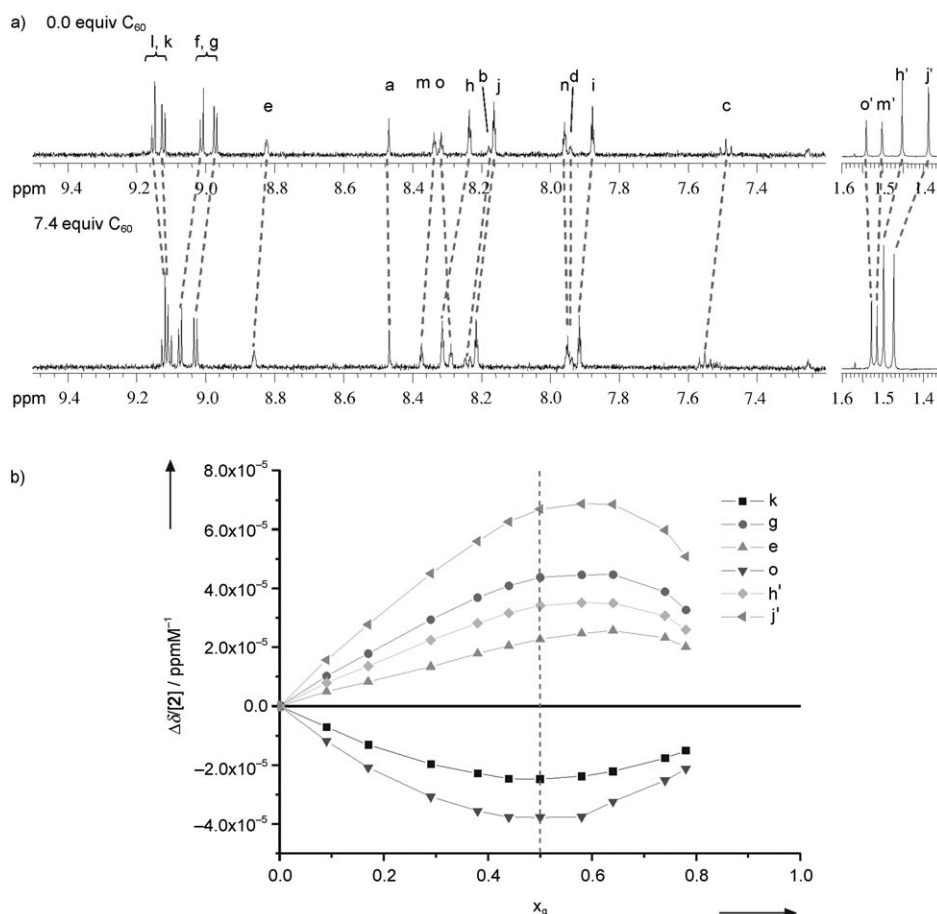


Figure 11. Titration of **2** ( $4.1 \times 10^{-4}$  M in [D<sub>8</sub>]toluene, constant concentration, 300 K) by C<sub>60</sub>. a) <sup>1</sup>H NMR chemical shift changes, b) Job plot for selected proton signals.

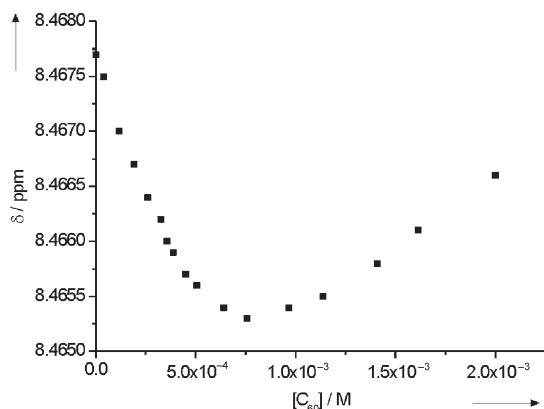


Figure 12. Chemical shift of proton *a* in **2** as a function of C<sub>60</sub> concentration.

## Conclusion

We have studied supramolecular assemblies of two porphyrin trimers and C<sub>60</sub> in the solid state and probed their solution behavior. Both complexes showed interesting binding geometries thanks to the presence of a third porphyrin in

the host molecule. For the smaller trimer **2**, a crystal structure with unusual fullerene–fullerene close contacts was observed and the supramolecular structure resulted from the formation of a one-dimensional porphyrin–fullerene chains. In solution, we interpret the <sup>1</sup>H NMR spectroscopic data as indicative of an unusual, bowl-shaped receptor conformation, binding to the fullerene guest with an association constant of 300 to 1000 M<sup>-1</sup>. The two effects can be explained by the fact that the smaller porphyrin trimer is not well-suited for any of the traditional porphyrin–fullerene binding modes.

In the case of the larger trimer host **1**, in toluene solutions, the intermolecular binding mode is not observed as expected, while the intramolecular binding mode is characterized by association constants of about  $2500 \pm 300$  M<sup>-1</sup>. Solid state data show the presence of one intramolecular complexation mode of C<sub>60</sub> by two parallel porphyrins, and discrete dimers

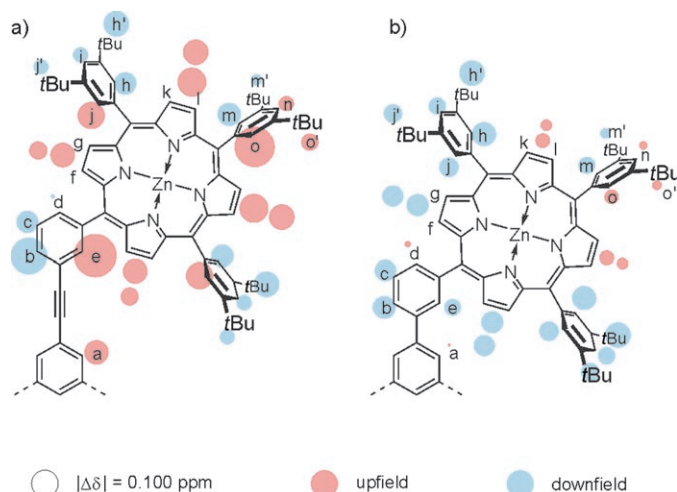


Figure 13. Schematic representation of chemical shift changes of protons of a) **1** and b) **2** upon complexation of C<sub>60</sub>.

of the porphyrin trimer, linked by C<sub>60</sub> molecules in the asymmetric unit, giving rise to a new supramolecular motif and surprisingly close porphyrin–fullerene distances.



The use of tripodal hosts as opposed to “porphyrin tweezers” dramatically influences the supramolecular behavior of hosts: $C_{60}$  complexes. While two of the porphyrin arms act as “tweezers” suitable for binding guests intramolecularly, the third arm provides intermolecular interactions resulting in formation of supramolecular networks. This work also brings evidence for the markedly different behavior in solution where the entropic penalty is too large to allow formation of supramolecular networks.

## Experimental Section

**General methods:**  $^1\text{H}$  NMR spectra were recorded at 300 K on a Bruker 500 MHz spectrometer fitted with a broadband ATM probe. Fluorescence spectra were recorded on a Cary Eclipse fluorimeter at an excitation wavelength of 420 nm.

**Materials:** Porphyrin trimers **1** and **2** were synthesized according to a published procedure.<sup>[20]</sup>  $C_{60}$  of 99.5% purity was purchased from Materials and Electrochemical Research Corporation.

**Porphyrin Trimer/ $C_{60}$  co-crystallizations:**  $C_{60}$  (2.1 mg, 2.9  $\mu\text{mol}$ ) and small trimer **1** (4.5 mg, 1.5  $\mu\text{mol}$ ) were mixed and dissolved in a minimum of toluene. Sonication and heating were necessary to assist the dissolution of fullerene. The mixture was then filtered and was carefully layered with hexane. The resulting mixture was left to stand undisturbed at room temperature and protected from light for several weeks, during which dark red crystals were obtained. Co-crystallizations of large trimer **2** (4.6 mg, 1.5  $\mu\text{mol}$ ) with  $C_{60}$  (2.1 mg, 2.9  $\mu\text{mol}$ ) were prepared following identical procedures and afforded dark red crystals.

**Crystal structure determination:** Crystallographic data of complexes **3** and **4** were collected on the synchrotron radiation source at Station 9.8, Daresbury SRS, UK, on a Bruker SMART CCD diffractometer. The structures were solved by direct methods using the program SIR92.<sup>[27]</sup> The refinement (on  $F$ ) and graphical calculations were performed using the CRYSTALS<sup>[28]</sup> program suite.

**Crystal data 3:**  $\text{C}_{222}\text{H}_{228}\text{N}_{12}\text{Zn}_3\cdot 4(\text{C}_{60})\cdot 2.75(\text{C}_6\text{H}_{14})\cdot 4.75(\text{C}_7\text{H}_8)\cdot 1.5\text{H}_2\text{O}$ :  $\text{C}_{717.75}\text{H}_{521}\text{N}_{24}\text{O}_{1.5}\text{Zn}_6$ ,  $M = 9874.47$ ,  $Z = 2$ , triclinic, space group  $P\bar{1}$ ,  $a = 28.947(6)$ ,  $b = 34.502(7)$ ,  $c = 35.097(7)$  Å,  $\alpha = 100.39(3)$ ,  $\beta = 109.41(3)$ ,  $\gamma = 110.52(3)^\circ$ ,  $V = 29161(17)$  Å<sup>3</sup>,  $T = 120(2)$  K,  $\mu = 0.3003$  mm<sup>-1</sup>. Of 131 046 reflections measured, 82 838 were independent ( $R_{\text{int}} = 0.047$ ). Final  $R = 0.1587$  (20 768 reflections with  $I > 3\sigma(I)$ ) and  $wR = 0.1892$ .  $\text{H}_2\text{O}$  hydrogens could not be found. The *t*Bu groups are all disordered, two were modeled over two positions, most have just been restrained. All solvent molecules are also disordered and have been idealized. The asymmetric unit contains two crystallographically unique trimers and four unique  $C_{60}$  molecules. Solvent and peripheral substituents have been removed. Figure 4 represents the essential part of two adjoining asymmetric units.

**Crystal data 4:**  $\text{C}_{210}\text{H}_{228}\text{N}_{12}\text{Zn}_3\cdot 2(\text{C}_{60})\cdot (\text{C}_6\text{H}_{14})\cdot 6(\text{C}_7\text{H}_8)$ :  $\text{C}_{378}\text{H}_{289}\text{N}_{12}\text{Zn}_3$ ,  $M = 5195.67$ ,  $Z = 2$ , triclinic, space group  $P\bar{1}$ ,  $a = 18.801(3)$ ,  $b = 26.501(4)$ ,  $c = 30.463(4)$  Å,  $\alpha = 88.038(2)$ ,  $\beta = 76.790(2)$ ,  $\gamma = 69.939(2)^\circ$ ,  $V = 13 864(4)$  Å<sup>3</sup>,  $T = 120(2)$  K,  $\mu = 0.322$  mm<sup>-1</sup>. Of 104 288 reflections measured, 48 672 were independent ( $R_{\text{int}} = 0.044$ ). Final  $R = 0.1426$  (19 863 reflections with  $I > 3\sigma(I)$ ) and  $wR = 0.1535$ . Asymmetric unit contains one porphyrin trimer and two independent  $C_{60}$  molecules. All *t*Bu groups were disordered, two were modeled as disordered over two positions. The solvent molecules are also disordered and have been idealized. Figure 7 represents the essential parts of four adjoining asymmetric units. Each  $C_{60}$  could be viewed as continuous sphere of electron density. Although this representation would better describe the disordered nature of this guest, this alternative refinement model did not give a significantly improved set of final parameters.

CCDC 660538, 660539 contain the supplementary crystallographic data for this paper. These data can be obtained free of charge from The Cambridge Crystallographic Data Centre via [www.ccdc.cam.ac.uk/data\\_request/cif](http://www.ccdc.cam.ac.uk/data_request/cif).

## Acknowledgements

This research was supported by EPSRC (L.H.T., J.L.W. and J.K.M.S.) and the Royal Society (S.I.P.). We acknowledge the EPSRC national crystallography service at Daresbury for synchrotron data collection of **2**. We thank Drs. A. Cowley (University of Oxford) and John E. Warren (SRS Daresbury) for assistance with crystallography.

- [1] L. R. Milgrom, *The Colours of Life: An Introduction to the Chemistry of Porphyrins and Related Compounds*, Oxford University Press, Oxford, UK 1997.
- [2] a) F. Wudl, *Acc. Chem. Res.* **1992**, *25*, 157–161; b) L. Echegoyen, L. E. Echegoyen, *Acc. Chem. Res.* **1998**, *31*, 593–601.
- [3] a) D. M. Guldi, M. Prato, *Acc. Chem. Res.* **2000**, *33*, 695–703; b) D. M. Guldi, *Chem. Commun.* **2000**, 321–327.
- [4] a) D. Kuciauskas, P. A. Liddell, S. Lin, T. E. Johnson, S. J. Weghorn, J. S. Lindsey, A. L. Moore, T. A. Moore, D. Gust, *J. Am. Chem. Soc.* **1999**, *121*, 8604–8614; b) C. Luo, D. M. Guldi, H. Imahori, K. Tamaki, Y. Sakata, *J. Am. Chem. Soc.* **2000**, *122*, 6535–6551; c) D. M. Guldi, *Chem. Soc. Rev.* **2002**, *31*, 22–36; d) H. Imahori, *Org. Biomol. Chem.* **2004**, *2*, 1425–1433; e) G. Kodis, Y. Terazono, P. A. Liddell, J. Andréasson, V. Garg, M. Hamburger, T. A. Moore, A. L. Moore, D. Gust, *J. Am. Chem. Soc.* **2006**, *128*, 1818–1827; f) F. D'Souza, S. Gadde, D.-M. S. Islam, C. A. Wijesinghe, A. L. Schumacher, M. E. Zandler, Y. Araki, O. Ito, *J. Phys. Chem. A* **2007**, *111*, 8552–8560.
- [5] a) S. R. Wilson, S. MacMahon, F. T. Tat, P. D. Jarowski, D. I. Schuster, *Chem. Commun.* **2003**, 226–227; b) P. D. W. Boyd, C. A. Reed, *Acc. Chem. Res.* **2005**, *38*, 235–242; c) T. Hasobe, H. Imahori, P. V. Kamat, T. K. Ahn, S. K. Kim, D. Kim, A. Fujimoto, T. Hirakawa, S. Fukuzumi, *J. Am. Chem. Soc.* **2005**, *127*, 1216–1228; d) F. D'Souza, R. Chitta, S. Gadde, L. M. Rogers, P. A. Karr, M. E. Zandler, A. S. D. Sandanayaka, Y. Araki, O. Ito, *Chem. Eur. J.* **2007**, *13*, 916–922; e) K. Tashiro, T. Aida, *Chem. Soc. Rev.* **2007**, *36*, 189–197.
- [6] a) T. Hasobe, Y. Kashiwagi, M. A. Absalom, J. Sly, K. Hosomizu, M. J. Crossley, H. Imahori, P. V. Kamat, S. Fukuzumi, *Adv. Mater.* **2004**, *16*, 975–979; b) M. Kimura, Y. Saito, K. Ohta, K. Hanabusa, H. Shirai, N. Kobayashi, *J. Am. Chem. Soc.* **2002**, *124*, 5274–5275.
- [7] a) T. Hasobe, H. Imahori, P. V. Kamat, S. Fukuzumi, *J. Am. Chem. Soc.* **2003**, *125*, 14962–14963; b) H. Imahori, S. Fukuzumi, *Adv. Funct. Mater.* **2004**, *14*, 525–536; c) H. Imahori, A. Fujimoto, S. Kang, H. Hotta, K. Yoshida, T. Umeyama, Y. Matano, S. Isoda, *Adv. Mater.* **2005**, *17*, 1727–1730; d) H. Imahori, A. Fujimoto, S. Kang, H. Hotta, K. Yoshida, T. Umeyama, Y. Matano, S. Isoda, M. Isosomppi, N. V. Tkachenko, H. Lemmetyinen, *Chem. Eur. J.* **2005**, *11*, 7265–7275; e) T. Hasobe, S. Hattori, P. V. Kamat, S. Fukuzumi, *Tetrahedron* **2006**, *62*, 1937–1946; f) H. Imahori, K. Mitamura, T. Umeyama, K. Hosomizu, Y. Matano, K. Yoshida, S. Isoda, *Chem. Commun.* **2006**, 406–408; g) H. Imahori, K. Mitamura, Y. Shibano, T. Umeyama, Y. Matano, K. Yoshida, S. Isoda, Y. Araki, O. Ito, *J. Phys. Chem. B* **2006**, *110*, 11399–11405; h) H. Imahori, *J. Mater. Chem.* **2007**, *17*, 31–41.
- [8] a) S. Yoshimoto, Y. Honda, Y. Murata, M. Murata, K. Komatsu, O. Ito, K. Itaya, *J. Phys. Chem. B* **2005**, *109*, 8547–8550; b) S. Zhang, L. Echegoyen, *Tetrahedron* **2006**, *62*, 1947–1954; c) D. Bonifazi, A. Kiebele, M. Stöhr, F. Cheng, T. Jung, F. Diederich, H. Spillmann, *Adv. Funct. Mater.* **2007**, *17*, 1051–1062.
- [9] D. Sun, F. S. Tham, C. A. Reed, P. D. W. Boyd, *Proc. Natl. Acad. Sci. USA* **2002**, *99*, 5088–5092.
- [10] a) D. V. Konarev, A. L. Litvinov, I. S. Neretin, N. V. Drichko, Y. L. Slovokhotov, R. N. Lyubovskaya, J. A. K. Howard, D. S. Yufit, *Cryst. Growth Des.* **2004**, *4*, 643–646; b) A. L. Litvinov, D. V. Konarev, A. Y. Kovalevsky, I. S. Neretin, P. Coppens, R. N. Lyubovskaya, *Cryst. Growth Des.* **2005**, *5*, 1807–1819.
- [11] a) M. M. Olmstead, D. J. Nurco, *Cryst. Growth Des.* **2006**, *6*, 109–113; b) A. Hosseini, M. C. Hodgson, F. S. Tham, C. A. Reed, P. D. W. Boyd, *Cryst. Growth Des.* **2006**, *6*, 397–403.

- [12] a) Y. Sun, T. Drovetskaya, R. D. Bolskar, R. Bau, P. D. W. Boyd, C. A. Reed, *J. Org. Chem.* **1997**, *62*, 3642–3649; b) M. M. Olmstead, D. A. Costa, K. Maitra, B. C. Noll, S. L. Phillips, P. M. Van Calcar, A. L. Balch, *J. Am. Chem. Soc.* **1999**, *121*, 7090–7097; c) D. V. Konarev, I. S. Neretin, Y. L. Slovokhotov, E. I. Yudanova, N. V. Drichko, Y. M. Shul'ga, B. P. Tarasov, L. L. Gumanov, A. S. Batsanov, J. A. K. Howard, R. N. Lyubovskaya, *Chem. Eur. J.* **2001**, *7*, 2605–2616; d) T. Ishii, N. Aizawa, R. Kanehama, M. Yamashita, K. Sugiura, H. Miyasaka, *Coord. Chem. Rev.* **2002**, *226*, 113–124.
- [13] P. D. W. Boyd, M. C. Hodgson, C. E. F. Rickard, A. G. Oliver, L. Chaker, P. J. Brothers, R. D. Bolskar, F. S. Tham, C. A. Reed, *J. Am. Chem. Soc.* **1999**, *121*, 10487–10495.
- [14] a) K. Tashiro, T. Aida, J.-Y. Zheng, K. Kinbara, K. Saigo, S. Sakamoto, K. Yamaguchi, *J. Am. Chem. Soc.* **1999**, *121*, 9477–9478; b) J.-Y. Zheng, K. Tashiro, Y. Hirabayashi, K. Kinbara, K. Saigo, T. Aida, S. Sakamoto, K. Yamaguchi, *Angew. Chem.* **2001**, *113*, 1909–1913; *Angew. Chem. Int. Ed.* **2001**, *40*, 1857–1861; c) A. L. Kieran, S. I. Pascu, T. Jarrosson, J. K. M. Sanders, *Chem. Commun.* **2005**, 1276–1278.
- [15] a) M. Ayabe, A. Ikeda, S. Shinkai, S. Sakamoto, K. Yamaguchi, *Chem. Commun.* **2002**, 1032–1033; b) Z.-Q. Wu, X.-B. Shao, C. Li, J.-L. Hou, K. Wang, X.-K. Jiang, Z.-T. Li, *J. Am. Chem. Soc.* **2005**, *127*, 17460–17468.
- [16] a) D. Sun, F. S. Tham, C. A. Reed, L. Chaker, M. Burgess, P. D. W. Boyd, *J. Am. Chem. Soc.* **2000**, *122*, 10704–10705; b) D. Sun, F. S. Tham, C. A. Reed, L. Chaker, P. D. W. Boyd, *J. Am. Chem. Soc.* **2002**, *124*, 6604–6612.
- [17] a) M. Ayabe, A. Ikeda, Y. Kubo, M. Takeuchi, S. Shinkai, *Angew. Chem.* **2002**, *114*, 2914–2916; *Angew. Chem. Int. Ed.* **2002**, *41*, 2790–2792; b) T. Yamaguchi, N. Ishii, K. Tashiro, T. Aida, *J. Am. Chem. Soc.* **2003**, *125*, 13934–13935.
- [18] A. Ouchi, K. Tashiro, K. Yamaguchi, T. Tsuchiya, T. Akasaka, T. Aida, *Angew. Chem.* **2006**, *118*, 3622–3626; *Angew. Chem. Int. Ed.* **2006**, *45*, 3542–3546.
- [19] D. M. Guldi, T. Da Ros, P. Braiuca, M. Prato, E. Alessio, *J. Mater. Chem.* **2002**, *12*, 2001–2008.
- [20] L. H. Tong, S. I. Pascu, T. Jarrosson, J. K. M. Sanders, *Chem. Commun.* **2006**, 1085–1087.
- [21] W. R. Scheidt, J. U. Mondal, C. W. Eigenbrot, A. Adler, J. Radonovich, J. L. Hoard, *Inorg. Chem.* **1986**, *25*, 795–799.
- [22] H. L. Anderson, J. K. M. Sanders, A. Bashall, K. Hendrick, M. McPartlin, *Angew. Chem.* **1994**, *106*, 445–447; *Angew. Chem. Int. Ed. Engl.* **1994**, *33*, 429–431.
- [23] M. Nakash, Z. Clyde-Watson, N. Feeder, S. J. Teat, J. K. M. Sanders, *Chem. Eur. J.* **2000**, *6*, 2112–2119.
- [24] M. Makha, A. Purich, C. L. Raston, A. N. Sobolev, *Eur. J. Inorg. Chem.* **2006**, 507–517.
- [25] K. Tsubaki, K. Tanaka, T. Kinoshita, K. Fujii, *Chem. Commun.* **1998**, 895–896.
- [26] P. Dauber, A. T. Hagler, *Acc. Chem. Res.* **1980**, *13*, 105–112.
- [27] A. Altomare, G. Carascano, C. Giacovazzo, A. Guagliardi, *J. Appl. Crystallogr.* **1993**, *26*, 343–350.
- [28] a) D. J. Watkin, C. K. Prout, J. R. Carruthers, P. W. Betteridge, *CRYSTALS* Issue 11, Chemical Crystallography Laboratory, Oxford UK, **2001**; b) P. W. Betteridge, J. R. Carruthers, R. I. Cooper, K. Prout, D. J. Watkin, *J. Appl. Crystallogr.* **2003**, *36*, 1487.

Received: October 25, 2007

Published online: February 21, 2008